Int. j. adv. multidisc. res. stud. 2022; 2(6):516-520

Received: 04-10-2022
Accepted: 14-11-2022

International Journal of Advanced Multidisciplinary Research and Studies

ISSN: 2583-049X

Estimation of a calibration relation of TDLS spectrometer to measure a gas concentration of NH_3 gas near-infrared region

[1] Ruaa Kahtan Mahmood, [2] Samira A Mahdi , [3] Amal Abd Al-Amir Al Masoudi
[1, 2, 3] Department of Physics, College of Sciences, University of Babylon, Babylon, 51001, Iraq

Corresponding Author: **Ruaa Kahtan Mahmood**

Abstract
A theoretical study has been implemented to enhance the detection limit of methane gas by tuning the wavelength of the open path tunable diode laser spectrometer (TDLS) in the near infrared region. MatLab code has been written to tune the accurate wavelength in the NIR region. Then, the frequency domain measurements have been carried out to extract the second harmonic as an indicator of gas existence. The results show the accurate wave length in NIR region is (1543.027 nm) and the measurement have been demonstrated at L = 100 m, the gas concentration was N = 0.05 to 0.5 ppb in 0.2 step for all gas measurement.

Keywords: TDLS, Ammonia Gas, Wavelength Tuning

1. Introduction

With the continuous development of industrialization, the application of ammonia (NH3) in industry has become more and more common, especially in the petrochemical industry, cold chain logistics, and fertilizer production. At the same time, traditional animal husbandry and agriculture are also important sources of ammonia emissions. SO2 and NO2 in the atmosphere react with NH3 under the action of water vapor to produce ammonium sulfate and ammonium nitrate particles. These particles are suspended in the atmosphere to form the PM2.5 aerosol, which is an important reason for the formation of haze [1, 2]. As a major chemical and agricultural production country around the world, China emits about 13.1 million tons of NH3 into the atmosphere each year, making it the largest NH3 emitter in the world [3]. Therefore, the development of an efficient, convenient, real-time, and high-precision NH3 remote sensor system is of great significance to improve the level of environmental protection and citizens' health.

As a key subject, researchers from various countries have proposed many methods to measure gas concentration [4, 5, 6, 7, 8, 9, 10, 11, 12]. As for the remote sensing of ammonia, Force *et al*. achieved the sensitivity of 5 ppb for atmospheric NH3 measurement by use of a CO2 differential absorption lidar system with the wavelength of 10.716 μm and 10.693 μm [13]; Theriault *et al*. designed a compact atmospheric sounding interferometer (CATSI) which could achieve the resolution of 40 ppm·m for NH3 remote sensing based on differential Fourier-transform infrared (FTIR) spectroscopy [14]; Dammers *et al*. did a lot of work on the research of the spatial distribution of NH3 with mini Differential Optical Absorption Spectroscopy (mini-DOAS) [15, 16, 17]. Dror *et al*. introduced an encoding–decoding method to improve spectral resolution when detecting various chemical species with Raman spectroscopy [18]. Comparing these methods, gas detection systems based on tunable diode laser absorption spectroscopy (TDLAS) technique have the merit of high resolution. However, traditional NH3 detection equipment based on TDLAS is usually deployed with a gas cell inside the device. Furthermore, NH3 will adhere to the pipeline and the system, which affects the accuracy, and the corrosion of pipelines also affects the life of the equipment. [19]. At the same time, the equipment deployed with a gas cell makes the testers inevitably exposed to the environment of NH3 leakage, which is not satisfactory from the perspective of industrial production. With the development of laser and waveguide technology, infrared laser beam can propagate over long distance after collimation. This is also the foundation for infrared laser remote sensing technology to achieve application [20].

In this paper, we propose a remote sensor system for NH3 leakage monitoring in the industrial production process based on the TDLAS technique. This system avoided deploying the gas cell which was usually used in traditional TDLAS sensor system. This change solved the problem caused by the adsorption and corrosion of the ammonia. Combined with the 2f/1f wavelength modulation spectroscopy (WMS) technique, this system suppressed the interference caused by the varied intensity and detection distance retained the merit of high resolution of TDLAS gas sensor system. To improve the refresh rate of digital system, we gave up the traditional "triangular wave + sine-wave" WMS scheme and adopted of "wavelength lock" scheme.

This change means the system can scan the absorption line of NH3 much more rapidly than the traditional TDLAS gas sensor. To realize the portability, we miniaturized this system into a handheld instrument. Considering the convenience of maintenance, later performance upgrade, and the cost of the system, we developed the digital lock-in amplification and 2f/1f signal processing program based on LabVIEW platform. We carried out a series of instrument performance characterization experiments and outdoor practical application tests, which verified the system has satisfactory performance. The NH3 remote sensor system has the advantages of simple structure, low cost, excellent portability, rapid response, remote no-contact measurement, and excellent anti-interference performance, which has promising application prospects.

According to the HITRAN database, H2O and CO2 in the atmosphere are the main interferences to the NH3 absorption line. For the remote sensor system, although the absorption intensity of NH3 molecules at 1512 nm nearby is several orders of magnitude higher than that of H2O and CO2 molecules [22], affected by the detection distance, the integral concentration of H2O molecules through the entire remote sensing range is much higher than that of NH3 molecules. Fig 1a shows the absorption spectra of NH3, H2O, and CO2 from 6550 cm−1 to 6650 cm−1 based on the HITRAN database. It is clearly shown that the absorption line at 6612.7 cm−1 is the strongest line of NH3 around the range and has no overlap with the absorption lines of H2O and CO2. Furthermore, it is a single-peak absorption line which satisfies the requirement of 2f/1f WMS signal processing theory. So, the characteristic absorption line at 1512.2 nm (wavenumber = 6612.7 cm−1) is selected as the wavelength of the remote sensing laser. Fig 1b shows the absorption intensity of 1000 ppm·m NH3, 600,000 ppm·m H2O and 18,000 ppm·m CO2 which are integral concentrations under the typical remote sensing distance of 30 m based on the HITRAN database. According to the data in Fig 1b, the absorption intensity of H2O and CO2 is much lower than that of NH3. Thus, the absorption intensity of H2O has no effect on the NH3 sensing results. Considering the absorption line of H2O at 6612 cm−1 interfering to the characteristic absorption line of NH3 at 6612.7 cm−1, the traditional "triangular wave + sine-wave" WMS scheme is abandoned and the "wavelength lock" scheme is adopted instead. This scheme is to fix the static output wavelength of a distributed feedback (DFB) laser at the center frequency and just modulate the output wavelength with a sinewave signal, which not only increases the sampling frequency, but also eliminates the interference of the H2O absorption line on the detection results [23].

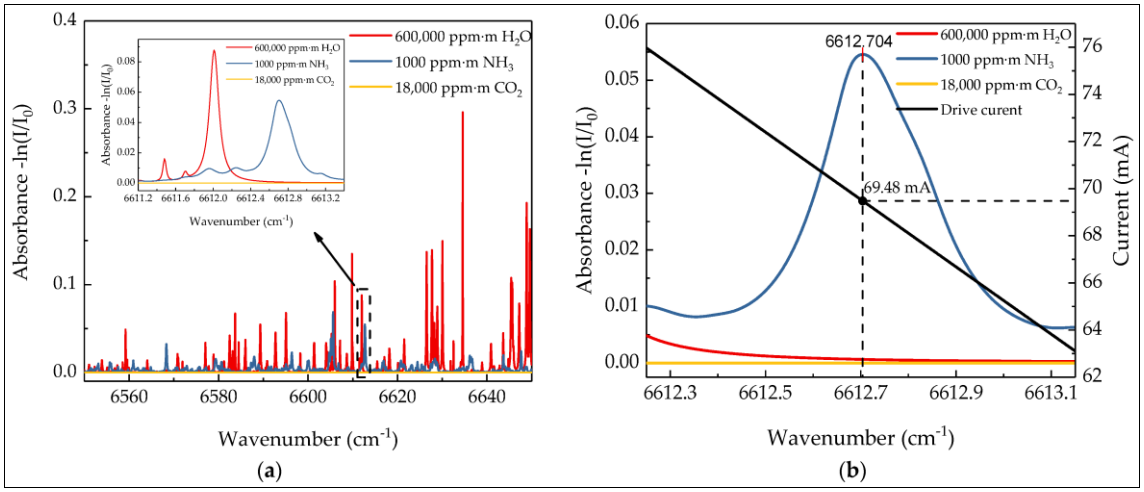

Fig 1: (a) Absorption spectra of NH3, H2O, CO2 from 6550 cm−1 to 6650 cm−1. (b) Absorption spectra of NH3 (1000 ppm·m, blue line), H2O (1%, red line), and CO2 (0.03%, yellow line) at an optical path of 60 m based on HITRAN database and the plot of drive current versus wavenumber of the distributed feedback (DFB) laser (black line), the value of modulation current at the central wavenumber 6612.7 cm−1 is 69.48 mA

2. Theory (Simulations)

The simulations of the light absorption by gases are based on the Beer-Lambert law [24]:

$$I = I_o e^{-\beta\sigma NL} \quad (1)$$

where Io is the fundamental incident intensity of IR laser light received by the photodiode when no gas is present. The incident intensity was modulated using sinusoidal waveform as shown in equation (2).

$$I_o = [(i_{offset} - i_{th}) + a \sin(2\pi f_o t)]\frac{\delta}{area} \quad (2)$$

where $i_{offset} = 99$ mA is the DC offset; $i_{th} = 19$ mA is the threshold current; $a = 42$ mA is the amplitude of the sine wave; $f_o = 500$ Hz is the modulation frequency; $\delta = 0.2055$ mW/mA is the differential efficiency (the direct relation constant that convert the laser current to the laser power); $area = 3.1$ mm^2 is the active area of the photodiode. A narrow bandwidth beam of the laser light was generated and swept through the absorption peak of methane, carbon monoxide gases.

Depending on the weather conditions in the Martian atmosphere, the pressure is only a few millibars, with a mean pressure of roughly 730 Pa = 7. 3 millibar [24]. Doppler broadening dominates and the line-shape of the absorption cross-section σ becomes Gaussian, as shown in equation (3).

$$\sigma = C\, e^{-\frac{(w_o + a\,\gamma \sin(2\pi f_o t) - w_p)^2}{2\varepsilon^2}} \quad (3)$$

If we substitute equation (2) and Eq. (3) in equation (1) we get:

$$I = [(i_{offset} - i_{th}) + a \sin(2\pi f_{mod} t)]\frac{\delta}{area} e^{-\beta NLC\, e} \frac{(w_o + a\gamma \sin(2\pi f_{mod} t) - w_p)^2}{2\varepsilon^2} \quad (4)$$

I_0 and I (mW/mm2) are the intensity of incident light and transmitted light, respectively; β is a factor to convert the unit from ppm to cm-3.

3. β Factor Calculation for Ammonia Gas:

We calculate β factor for Ammonia gas as follow:

$\beta = 1\ ppm = \frac{1mg}{L} = \frac{10^{-3}\ g}{10^3\ M\ cm^3}$, where M is the molecular weight of ammonia gas, so $c = \frac{10^{-6}\ g}{\frac{17.031\ g}{mol} cm^3} = 0.059 \times \frac{10^{-6}\ mol}{cm^3} \times N_A$, NA is the Avogadro number (cm-3/ppm), As a result, $\beta = 0.059 \times \frac{10^{-3}\ mol}{cm^3} \times 6.022 \times 10^{20} \frac{1}{mol} = 0.355 \times \frac{10^{-3}}{cm^3} \times 10^{20} = 0.355E17$, and; N (parts per million) is the gas concentration; and $L = 100$ m is the light path length through the gas. In equation (4), C = 1E-20 cm2 is the cross-section area of the absorption peak of ammonia gas and its variance $\varepsilon = 0.1$ nm over the wavelength range which appears in the term of $(w_o + a\gamma \sin(2\pi f_o t) - w_p)$. $w_o = 1543$ nm in NIR $w_o = 2399$ nm in mid IR is the initial value of the scanning wavelength of the diode laser; $a\gamma \sin(2\pi f_o t)$ is the AC current waveform used to adjust the wavelength of emitted light from the laser, with $a = 42$ mA is the amplitude of the sine wave; $\gamma = 0.01$ nm/mA is a modulation factor; fo = 500 Hz is the modulation frequency; t is time in seconds; FWHM = 0.24 nm [25] in NIR; FWHM = 0.33 nm [26] in MIR is a full width half maximum; and $w_p = 1543.4$ nm [25] $w_p = 2399.9$ nm [27] is the peak value of the absorption spectrum of ammonia gas in near and mid infrared region; respectively.

4. Results and discussion

For Ammonia Gas Absorption Peak in The NIR Spectral Region

Fig 2 shows the absorption signal of the ammonia gas at tuning current of laser diode 86.01mA and the wavelength 1543.027 nm. The dip of the absorption peak locates exactly at the middle of the sine wave, and it is a deep and sharp dip. That means there was a highly sense of ammonia gas for that specific wavelength 1543.027 nm, and the frequency of the laser light has been matching vibrational frequencies of the ammonia gas at this wavelength. Note that the concentration of ammonia gas has been fixed at 0.5 ppb and the length of the open path spectrometer was fixed at 100 m.

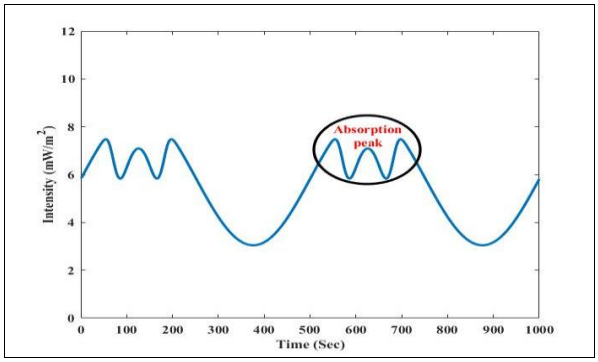

Fig 2: Ammonia absorption peak in near infrared region at tuning current of laser diode (86.01mA) and the wavelength (1543.027 nm)

Absorption signal in time domain has been plotted as shown in Fig 3. It is obvious there is no clear absorption signal as compare as with Fig 2 Because the wavelength of the laser passes out the matching point of the vibrational energy states that can be absorb the energy of the light laser beam.

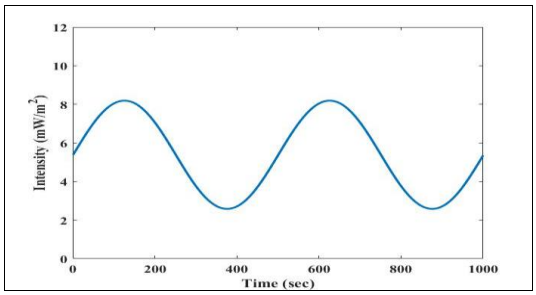

Fig 3: Absence of ammonia absorption peak in near infrared region at tuning current of laser diode (88.35 mA) and wave length (1543.051 nm)

A fast Fourier transformation (FFT) has been implemented to extract the second harmonic as an indicator for the gas presence that written done by MATLAB code. Fig 4 shows the chart of the fast Fourier Transmission (FFT) for the time domain data that exhibit in fig 2 where the fundamental frequency located at 500 Hz and the second harmonic has been indeed in the 1000 Hz also the value of the second harmonic seems to be significant 0. 33 mW/m2 that mean the energy of light has been mostly absorb.

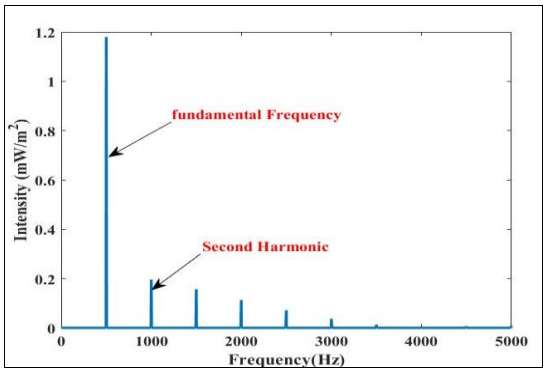

Fig 4: Fundamental frequency of ammonia gas in near infrared region at 500 Hz and the absorption peak at 1000 Hz

The result in fig 5 exhibits the fundamental frequency and the value of second harmonic, it seems that the second harmonic has been diminished (there is no absorption peak).

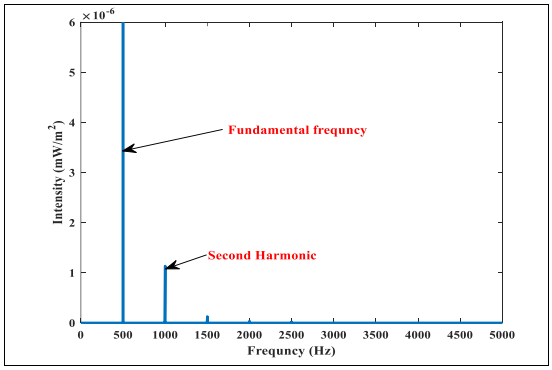

Fig 5: Fundamental frequency of ammonia gas in near infrared region at 500 Hz and the amount of the second harmonic reached about zero at1000 Hz

A MATLAB code has been written to evaluate the amount at the operation current of laser diode (LD) that can be give a max second harmonic value and it was found that the relation has max. peak and min. valley at current values 86.01 mA, 88.35 mA, respectively as shown in fig 6.

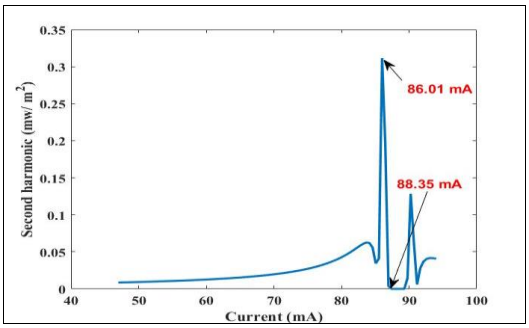

Fig 6: Variation of the second harmonic with the tuning current of ammonia gas in near infrared region

Then the spectrum wavelength has been tuned around 1nm in 0.02 nm steps to increase the sensitivity of the tunable diode spectrometer (TDLS). And it was the main goal of this work. as illustrate in fig 7 and it was found the relation has maximum peak and minimum valley at was wavelength values1543.027 nm, 1543.051 nm, respectively in near infrared that was done by MATLAB code.

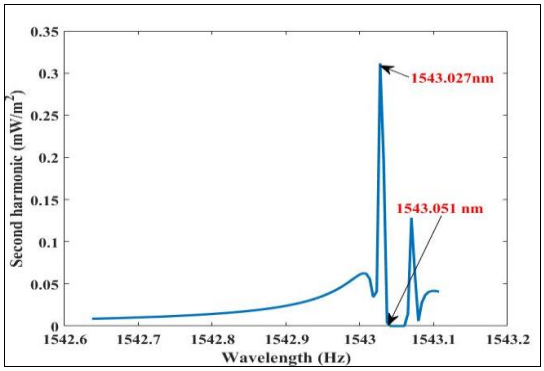

Fig 7: The wavelength spectrum of ammonia gas in near infrared region has a one peak at (1543.027 nm)

Fig 8 shows the relation between the second harmonic and the gas concentration at desired value of the driven current of the laser diode and at exact wavelength the 1543.027 nm the relation seems to be linear and the gas concentration's minimum value was 0.05 ppb.

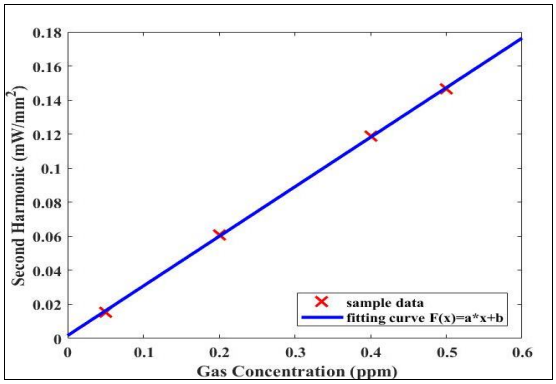

Fig 8: Relation between second harmonic and gas concentration of ammonia gas in near infrared region

5. Conclusions

In this work the simulation process of TDLS has been implemented to enhance the sensitivity of the spectrometer by modulating the wavelength of a DFB tunable laser diode using a sinusoid signal. The drive current of the laser has been tuned, therefore the wavelength of the laser diode will be change in tuning limits reach about 0.02 nm in NIR region. That was done to evaluate the sensitivity of the TDLS spectrometer in these ranges of spectrum frequencies. the NH_3 gas the simulation measurements have been showed a same min. limit of the gas concentration but under different values of wavelength of DFB tunable laser diode. Where in NIR region the accurate wavelength was 1543.027 nm with drive was about 86.01 mA.

6. References

1. Li SW, Chang MH, Li HM, Cui XY, Ma LQ. Chemical compositions and source apportionment of PM2.5 during clear and hazy days: Seasonal changes and impacts of Youth Summer Olympic Games. Chemosphere. 2020; 256:127163. [Google Scholar] [Cross Ref]
2. Wang P, Cao JJ, Shen ZX, Han YM, Lee SC, Huang Y, *et al*. Spatial and seasonal variations of PM 2.5 mass and species during 2010 in Xi'an, China. Sci. Total Environ. 2015; 508:477-487. [Google Scholar] [Cross Ref] [PubMed]
3. Kong L, Tang X, Zhu J, Wang Z, Pan Y, Wu H, *et al*. Improved Inversion of Monthly Ammonia Emissions in China Based on the Chinese Ammonia Monitoring Network and Ensemble Kalman Filter. Environ. Sci. Technol. 2019; 53:12529-12538. [Google Scholar] [Cross Ref] [PubMed]
4. Hodgkinson J, Tatam RP. Optical gas sensing: A review. Meas. Sci. Technol. 2012; 24:012004. [Google Scholar] [Cross Ref] [Green Version]
5. Guth U, Vonau W, Zosel J. Recent developments in electrochemical sensor application and technology: A review. Meas. Sci. Technol. 2009; 20:91. [Google Scholar] [Cross Ref]
6. Kwak D, Lei Y, Maric R. Ammonia gas sensors: A comprehensive review. Talanta. 2019; 204:713-730. [Google Scholar] [Cross Ref] [PubMed]
7. Salem AA, Soliman AA, El-Haty IA. Determination of nitrogen dioxide, sulfur dioxide, ozone, and ammonia in ambient air using the passive sampling method associated with ion chromatographic and potentiometric analyses. Air Qual. Atmos. Health. 2009; 2:133-145. [Google Scholar] [Cross Ref][Green Version]
8. Miller DJ, Sun K, Tao L, Khan MA, Zondlo MA. Open-path, quantum cascade-laser-based sensor for high-resolution atmospheric ammonia measurements. Atmos. Meas. Tech. 2014; 7:81-93. [Google Scholar] [Cross Ref] [Green Version]
9. He Y, Jin C, Kan R, Liu J, Liu W, Hill J, *et al*. Remote open-path cavity-ringdown spectroscopic sensing of trace gases in air, based on distributed passive sensors linked by km-long optical fibers. Opt. Express. 2014; 22:13170-13189. [Google Scholar] [Cross Ref]
10. Tao L, Sun K, Miller DJ, Pan D, Golston LM, Zondlo MA. Low-power, open-path mobile sensing platform for high-resolution measurements of greenhouse gases

and air pollutants. Appl. Phys. A. 2015; 119:153-164. [Google Scholar] [Cross Ref]
11. Guo X, Zheng F, Li C, Yang X, Li N, Liu S, *et al*. A portable sensor for in-situ measurement of ammonia based on near-infrared laser absorption spectroscopy. Opt. Lasers Eng. 2019; 115:243-248. [Google Scholar] [CrossRef]
12. Vasileiadis M, Athanasekos L, Meristoudi A, Alexandropoulos D, Mousdis G, Karoutsos V, *et al*. Diffractive optic sensor for remote-point detection of ammonia. Opt. Lett. 2010; 35:1476-1478. [Google Scholar] [CrossRef]
13. Force AP, Killinger DK, Defeo WE, Menyuk N. Laser remote sensing of atmospheric ammonia using a CO_2 lidar system. Appl. Opt. 1985; 24:2837-2841. [Google Scholar] [CrossRef]
14. Thériault J, Puckrin E. Remote sensing of chemical vapours by differential FTIR radiometry. Int. J. Remote. Sens. 2005; 26:981-995. [Google Scholar] [Cross Ref]
15. Dammers E, Vigouroux C, Palm M, Mahieu E, Warneke T, Smale D, *et al*. Retrieval of ammonia from ground-based FTIR solar spectra. Atmos. Chem. Phys. Discuss. 2015; 15:12789-12803. [Google Scholar] [CrossRef] [Green Version]
16. Dammers E, Palm M, Damme MV, Vigouroux C, Smale D, Conway S, *et al*. An evaluation of IASI-NH3 with ground-based FTIR measurements. Atmos. Chem. Phys. 2016; 16:1-30. [Google Scholar] [CrossRef][Green Version]
17. Dammers E, Schaap M, Haaima M, Palm M, Kruit RJW, Volten H, *et al*. Measuring atmospheric ammonia with remote sensing campaign: Part 1-Characterisation of vertical ammonia concentration profile in the centre of The Netherlands. Atmos. Environ. 2017; 169:97-112. [Google Scholar] [CrossRef]
18. Malka D, Berkovic G, Hammer Y, Zalevsky Z. Super-Resolved Raman Spectroscopy. Spectrosc. Lett. 2013; 46:307-313. [Google Scholar] [Cross Ref]
19. Pogány A, Balslev-Harder D, Braban CF, Cassidy N, Ebert V, Ferracci V, *et al*. A metrological approach to improve accuracy and reliability of ammonia measurements in ambient air. Meas. Sci. Technol. 2016; 27:115012. [Google Scholar] [CrossRef] [Green Version]
20. Moshaev V, Leibin Y, Malka D. Optimizations of Si PIN diode phase-shifter for controlling MZM quadrature bias point using SOI rib waveguide technology. Opt. Laser Technol, 2021; 138:106844. [Google Scholar] [CrossRef]
21. Modugno G, Corsi C. Water vapour and carbon dioxide interference in the high sensitivity detection of NH_3 with semiconductor diode lasers at 1.5 μm. Infrared Phys. Technol. 1999; 40:93-99. [Google Scholar] [CrossRef
22. Modugno G, Corsi C. Water vapour and carbon dioxide interference in the high sensitivity detection of NH_3 with semiconductor diode lasers at 1.5 μm. Infrared Phys. Technol. 1999; 40:93-99. [Google Scholar] [Cross Ref]
23. Houghton JT. The physics of atmospheres (2nd ed., Cambridge University Press, 1986), Cambridge, page 271. A Remote Sensor System Based on TDLAS Technique for Ammonia Leakage Monitoring.
24. Houghton J. The physics of atmospheres. Cambridge University Press, 2002.
25. Mahdi SA. An investigation of electro-optical 1/f noise reduction in an open-path tunable diode laser spectrometer (Doctoral dissertation, University of Arkansas at Little Rock), 2013.
26. Milton Filho B, da Silva MG, Sthel MS, Schramm DU, Vargas H, Miklós A, *et al*. (2006). Ammonia detection by using quantum-cascade laser photoacoustic spectroscopy. Applied optics, 45(20), 4966-4971.
27. Popa D, Udrea F. Towards integrated mid-infrared gas sensors. Sensors. 2019; 19(9):2076.